PROCEEDINGS, 42nd Workshop on Geothermal Reservoir Engineering
Stanford University, Stanford, California, February 13-15, 2017
SGP-TR-212

Improved image of intrusive bodies at Newberry Volcano, Oregon, based on 3D gravity modelling

Alain Bonneville[1], Trenton T. Cladouhos[2], Kelly Rose[3], Adam Schultz[4]

Chris Strickland[1], Scott Urquhart[5]

[1]Pacific Northwest National Laboratory, 902 Battelle Blvd, PO Box 999, Richland, WA 99352

[2]AltaRock Energy Inc., 4010 Stone Way N, Suite 400, Seattle, WA 98103

[3]National Energy Technology Laboratory, Albany, OR 97331-5503

[4]Oregon State University, 104 CEOAS Administration Building, Corvallis, OR 97331-5503

[5]Zonge International, 3322 East Fort Lowell Road, Tucson, Arizona 85716

alain.bonneville@pnnl.gov; tcladouhos@altarockenergy.com; Kelly.Rose@netl.doe.gov; adam.schultz@oregonstate.edu; Christopher.Strickland@pnnl.gov; Scott.Urquhart@zonge.com

Keywords: Newberry, EGS, Cascade Range, Gravity

ABSTRACT

Beneath Newberry Volcano is one of the largest geothermal heat reservoirs in the western United States and it has been extensively studied for the last 40 years. Several magmatic intrusions have been recognized at depths between 2.5 and 8 km and some of them identified as suitable targets for enhanced geothermal energy and tested during two previous EGS campaigns. These subsurface structures have been intersected by three deep wells and imaged by various geophysical methods including seismic tomography and magnetotellurics. Although three high quality gravity surveys were completed between 2006 and 2010 as part of various projects, a complete synthesis and interpretation of the gravity data has not yet been performed. Regional gravity data also exist in the vicinity of the Newberry volcano and have been added to these surveys to constitute a dataset with a total of 1418 gravity measurements. When coupled with existing geologic and geophysical data and models, this new gravity dataset provides important constraints on the depth and contours of the magmatic bodies previously identified by other methods and thus greatly contributing to facilitate any future drilling and stimulation works.

Using the initial structures discovered by seismic tomography, inversion of gravity data has been performed. Shape, density values and depths of various bodies were allowed to vary and three main bodies have been identified. Densities of the middle and lower intrusive bodies (~2.6-2.7 g/cm3) are consistent with rhyolite, basalt or granites. Modeled density of the near-surface caldera body match that of a low density tephra material and the density of the shallow ring structures contained in the upper kilometer correspond to that of welded tuff or low-density rhyolites. Modeled bodies are in reality a composite of thin layers; however, average densities of the modeled gravity bodies are in good agreement with the density log obtained in one well located on the western flank (well 55-29). Final gravity data residuals show that most of the observed gravity anomalies at the surface can be explained by the modeled gravity bodies and are consistent with other site characterization information.

1. INTRODUCTION

Newberry Volcano is situated near the juncture of several geologic provinces in central Oregon: the Cascade Range and volcanic arc to the west, the Columbia River Basalt Plateau to the northeast, and the Basin and Range to the southeast. The Cascade Arc created by the subduction of the Juan de Fuca plate under the North American plate is a long-lived feature with a magmatic history including several prominent eruptive periods, the Western Cascades from 35-17 Ma, the early High Cascades from 7.4 to 4.0 Ma, and the late High Cascades from 3.9 Ma to present (Priest, 1990).

Thanks to extensive geologic and geothermal exploration data collected over the past 40 years from Newberry Volcano and the surrounding region the Newberry volcano history and structure is quite well known. In particular, three large projects funded by the U.S. Department of Energy (DOE) have been performed since 2008. AltaRock Energy, Inc. (Altarock) led the Newberry EGS Demonstration project (NEGSD) (Cladouhos et al., 2015), Davenport Newberry Holdings (DNH, now part of AltaRock), led an Innovative Exploration Technology project (Waibel et al., 2015), and finally Oregon State University (OSU) with the National Energy Technology Laboratory (NETL) and Zonge International carried out a four-dimensional (4D) EGS monitoring project to complement the NEGSD (Mark-Moser et al., 2016). Newberry Volcano has been demonstrated to be extremely favorable for EGS technologies and the development of EGS reservoirs. Four deep, high-temperature production wells have been drilled in the area, along with a number of temperature gradient and core holes. Finally, this site was selected as a candidate for the DOE FORGE Phase in 2015 and a comprehensive synthesis of its geology has been produced (NEWGEN Phase 1 Topical Report and Geological Model, https://energy.gov/eere/forge/downloads/pacific-northwest-national-laboratory-phase-1-report). The gravity data processing and interpretation presented in this paper have been completed during this phase.

2. GEOLOGY AND MAIN STRATIGRAPHIC UNITS

Newberry Volcano is a broad eruptive center active for approximately the last 600,000 years that rises 2,408 m on the southeastern side of the Deschutes Basin (MacLeod et al., 1982; Jensen, 2006). The volcano is an elliptical shaped massif approximately 50 km by 30 km with some lava flows reaching more than 64 km north of the caldera (Figure 1). The lower flanks are composed of ash and lahar deposits, basaltic lava, cinder cones, and minor silicic domes. Several basalt flows sourced from rifts in the NW flank of the edifice are younger than 7,000 years, coeval with the regionally extensive Mazama ash. The more steeply sloped upper flanks of the volcano are composed predominantly of overlapping silicic domes and subordinate basaltic rock. The central caldera is about 8 km by 5 km and is a nested composite of craters and vents. The central caldera contains two lakes, Paulina Lake on the west at an elevation of 1,930 m and East Lake on the east at an elevation of 1,941 m. Within the caldera are resurgent obsidian flows, cinder cones, and maars, with the most recent eruption, which produced the Big Obsidian flow and ash fall dated at 1310 ^{14}C yr BP (Jensen 2006). The elevation of the rim of the caldera ranges from 2,133-2,408 m, except along the breached western side, where the elevation is 1,929 m.

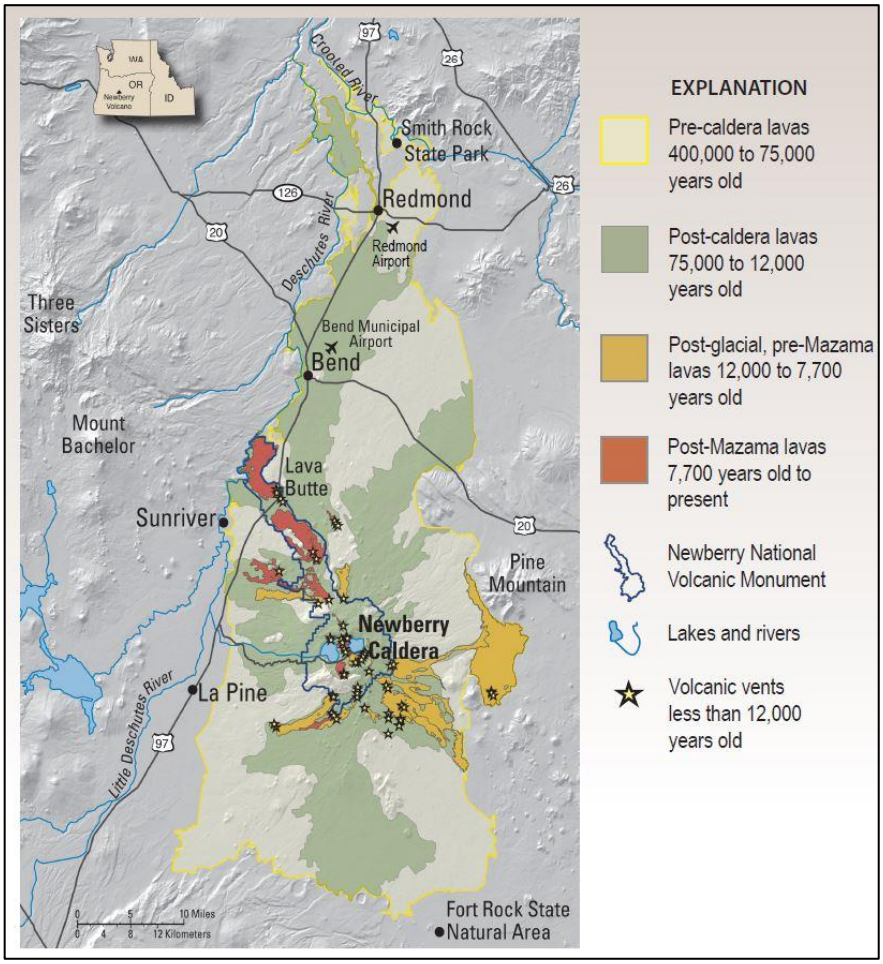

Figure 1. Lava flows and young volcanic vents at Newberry Volcano (from Donnelly-Nolan et al. 2011).

Newberry volcanic rocks are built upon the regionally extensive Pliocene Deschutes Formation (>7-4 Ma), which includes basalt flows, andesite flows, debris flows, ash-flow tuffs, ignimbrites, rhyolite and rhyodacite, and eroded and reworked basaltic and andesitic volcanic sediments. Beneath the Deschutes Formation, older volcanic, sedimentary, and tuffaceous rocks of the John Day, Mescal, and Clarno formations are either encountered or inferred.

Analyses of surface rock samples show a wide range of igneous rock compositions, dominated by a bimodal concentration of basaltic andesite and rhyodacite. Hundreds of volcanic vents and fissures are located on and adjacent to the volcano, some of which pre-date Newberry. Data from MacLeod et al. (1982), and from deeper temperature coreholes, suggest that the early eruptive history of the edifice was dominated by mafic lava. Over time, the magmatic character changed to the current bimodal basaltic andesite and rhyodacite. The Newberry flows are deposited on older volcanic and clastic sequences, most of which do not outcrop locally. In particular, below 2000 m depth beneath the surface, the Oligocene John Day Formation (37-19 Ma) which is composed of silicic, intermediate, and basaltic volcanic lava flows, rhyolite ash-flow tuff, and dacite to rhyodacite tuffs and alluvial deposits, (Robinson et al., 1984) is intruded by many sills and dykes coming from the main magma chamber. While existing wellbores extend to ~3000

m depth, number of dykes and plutonic bodies at depths greater than 3000 m beneath the west flank can only be inferred from geophysical data.

Four deep exploratory wells have been drilled on the northwestern flank of the volcano, two by CalEnergy (CEE 86-21 and CEE 23-22) and two by DNH (NWG 55-29 and NWG 46-16). The temperature profile for NWG 55-29 indicates a conductive regime with an equilibrated conductive temperature gradient of 109–128°C/km from 338 m to the bottom of the well at 3100 m depth.

3. SEISMIC TOMOGRAPHY

Beachly et al. (2012) represents the most comprehensive seismic *P-wave* velocity model of Newberry Volcano published to date. This study made use of data from a series of high-resolution explosive source seismic profiles obtained at Newberry Volcano in 1983 and 1984 by the USGS, and by a team from the University of Oregon in 2008.

The 3D seismic tomographic velocity model (Figure 2) shows at shallow depths that a ring-shaped high-velocity anomaly underlies the caldera ring faults that were previously identified by MacLeod et al. (1995). This 7 km by 5 km wide, 1 to 2 km laterally thick ring structure surrounds a central low-velocity zone that extends from 0.5 km to 2 km beneath the caldera. Beneath this, *P-wave* velocities in the ring structure increase, and the structure widens, particularly to the west and east of the caldera. At 3 km depth, the eastern high-velocity anomaly is 1 km/s faster than average, and the western is 0.6 km/s faster. Beneath 3 km, the high velocity widens further, although the extent is poorly resolved.

The tomographic model reveals a heterogeneous seismic velocity structure beneath the volcano. The heterogeneities may not map simply to changes in lithology, but may also reflect variations in porosity and temperature, and also the presence of partial melt at depth beneath the caldera. The low-velocity zone within the caldera is inferred to be porous, caldera-fill deposits in the upper 500 m, and from 500 m to 2 km beneath the caldera low velocities are associated with porous, fractured lava flows that correlate with those identified in drill cores (Beachly et al. 2012).

Additionally, the presence of partial melt beneath Newberry Volcano provides an enormous store of heat; the three preferred models predict a range of melt volumes between 1.6 and 8.0 km^3 (Beachly et al. 2012). Frone et al. (2014) estimate that there is 6.1 EJ (exajoules)
[10^{18} joules]) of heat contained within the upper 3.5 km beneath the caldera, and 174.4 EJ beneath the entire volcanic edifice, to that same depth.

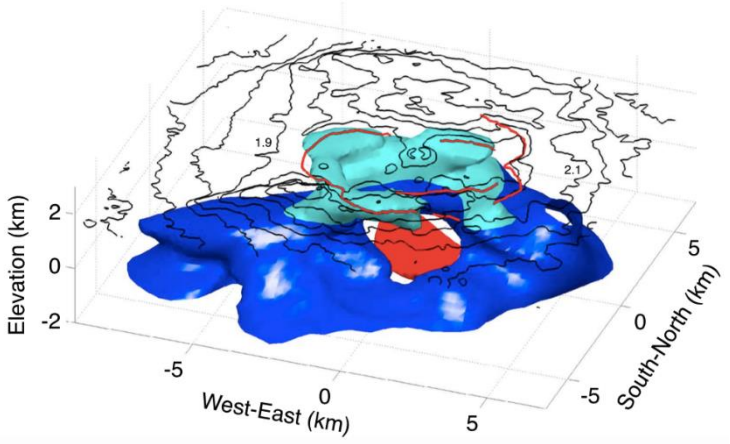

Figure 2. 3D seismic travel-time tomographic model of P-wave velocity beneath Newberry Volcano. High-velocity structure is light blue above 1.5 km depth and dark blue beneath that. The high-velocity isosurfaces represent intervals of +0.2 km/s velocity above a background 1D structure. The difference in shade of blue illustrates a possible structural difference between a shallow high-velocity ring structure associated with the caldera rim, and a broader, deeper high-velocity region. A central low-velocity region appears in red, shown as a -0.1 km/s velocity perturbation isosurface from the 3 to 5 km depth. A shallow low-velocity anomaly within the caldera is not shown. Red lines at the surface are inferred ring fractures; black lines show 0.1 km topographic contours. (From Beachly et al. 2012.)

These tomographic results have been used as a starting point for the gravity modelling and interpretation.

4. GRAVITY

Three gravity surveys were completed from 2006 to 2010 by Zonge International. In addition to the Zonge surveys, publicly available gravity data for the vicinity of Newberry Volcano (Roberts et al. 2008) were included in the overall data set. A total of 1418 gravity measurement locations were recorded for this analysis (Figure 3). A brief description of the surveys and preliminary data processing is presented here; more details can be found in previous reports (Zonge 2007, 2010, and 2012). The instrumentation

used consists of a LaCoste and Romberg model G gravimeter and Leica Geosystems survey-grade Global Positioning System (GPS)/Global Navigation Satellite System receivers.

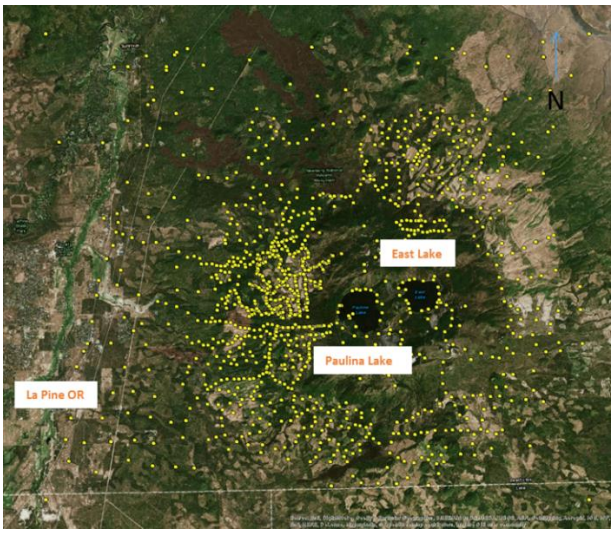

Figure 3. Locations of the gravity stations used in the analysis

4.1. Gravity Data Pre-Processing

Gravity measurements are affected by several factors and each must be accounted for in order to provide the highest quality results. The LaCoste and Romberg model G is capable of measuring microGal (~10^{-8} m/s^2) level acceleration variations of the Earth's gravitational field with an established resolution and repeatability of 10 μGal. The gravitational field varies with the distance from the center of the Earth and thus the elevation of the instrument affects the gravity measurement. A free-air correction accounts for the contribution of the instrument elevation and is an initial step in processing gravity data after corrections for instrument drift and Earth tides have been performed. Centimeter vertical position accuracy is required to achieve a μGal level accuracy in the free-air corrected gravity readings. Real-Time Kinematic (RTK) mode GPS surveys were performed by simultaneously collecting carrier-phase GPS data at individual gravity stations and at a fixed base station location. RTK mode assists with evaluating position solution quality in the field. Repeat gravity and GPS data were also acquired at a subset of stations and observed data errors were approximately 22 μGal and 20 cm respectively.

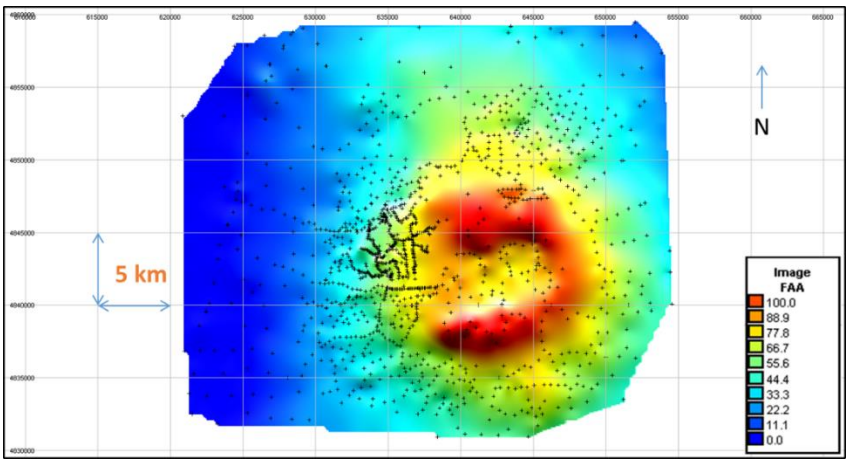

Figure 4. Free-air anomaly map. . Color map units are in mGal. Crosses correspond to location of the gravity stations used in the analysis.

The free-air gravity anomaly data are shown in Figure . Gravity data are often further reduced using the Bouguer correction method that aims to correct for any additional mass between the gravimeter and mean sea level. The approach followed here is instead to directly model the gravitational response of both the surface topography and subsurface structures and not rely on simplifying assumptions inherent in Bouguer corrections (Clouard et al., 2000).

4.2. Gravity Forward Modeling

Gravity modeling analysis was performed using ENcom Model Vision™ 12.0, a 3D numerical modeling software. Surface topography can be accurately measured and serves as the uppermost bounding surface of the first body included in the gravity modeling. For this analysis, a digital elevation map with a 100 m spaced grid was used to describe the surface topography. The elevation map was digitized using triangular elements to numerically define the upper surface of the gravity model. A shallow geological formation was defined from the upper surface down to 1250 m above sea level (ASL) and given a density of 2.3 g/cm^3.

The gravitational response of this formation can then be modeled and compared to the observed gravity data. Subtracting the modeled from the observed data provides an image of the data residual and is subsequently used to guide selection of additional subsurface structures that will be needed to better fit the observations. Data residuals after modeling the surface structure are shown in ***Figure*** and it is apparent that the modeled data are generally under predicted below the volcano except very near the center. Several ring like structures surround the center and would be consistent with other geologic evidence at the site.

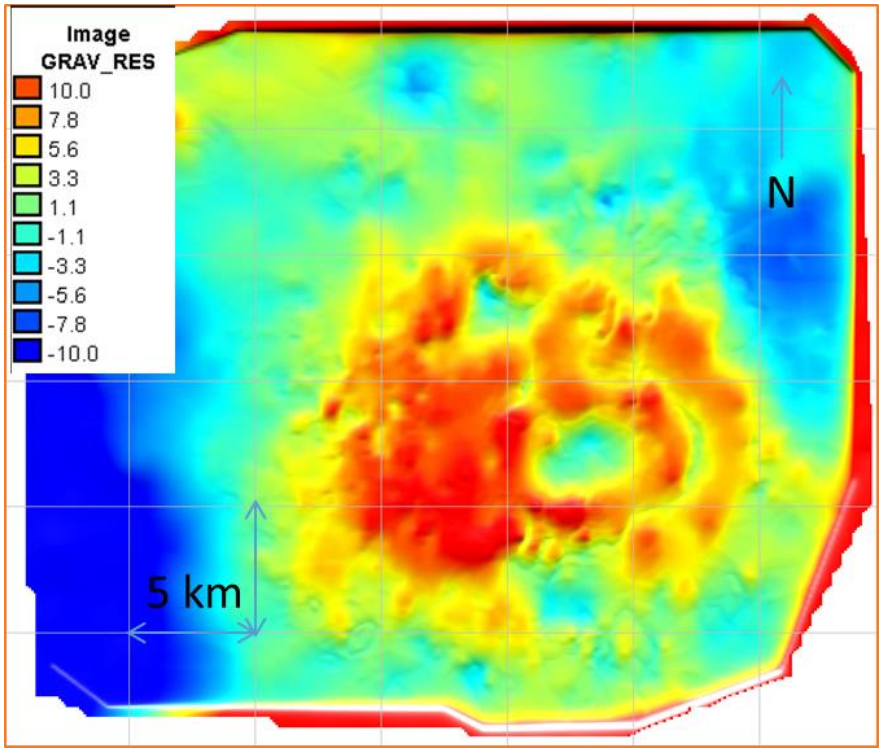

Figure 5. Data residual map showing the difference between modeled and observed data. Color map units are in mGal and the color scale is reduced compared to Figure 4.

Additional subsurface structures were added to improve the fit between the modeled and observed data. In addition to the surface topography residual gravity data, results from the seismic tomography performed at the site (see section 3) were used to guide the design of additional subsurface structures for inclusion in the gravity modeling. The set of modeled gravity body consists of a single shallow body near the center of the caldera, four shallow ring structures, two mid-depth intrusive bodies, and one deep intrusive body.

4.3. Gravity Inversion

Based on the initial forward model, inversion of the gravity data was performed allowing the density values and depths of the different bodies to vary. The free parameters were adjusted to minimize the errors between modeled and observed gravity values.

Three main bodies with similar densities can be identified and they are represented in Figure 6. The corresponding model parameters are listed in Table 1 with the same color. Densities of the middle and lower intrusive bodies (~2.6 to 2.7 g/cm^3) are consistent with rhyolite, basalt, or granites. The modeled density of the near-surface caldera body matches that of a low-density tephra material and the density of the shallow ring structures contained in the upper kilometer corresponds to that of welded tuff or low-density rhyolites.

Table 1. Gravity modeling parameters for each of the subsurface structures (colors are the ones used to represent the different structures in Figure 6 and 7).

Name	Depth at well NWG 55-29 (m bgs)	Thickness (m)	Density Anomaly (g/cm^3)	Background density (g/cm^3)	Density (g/cm^3)
Terrain	0-1300	-	0.00	2.30	2.30
Caldera_NS	-	500	-0.35	2.30	1.95
Ring_North	-	800	0.12	2.30	2.42
Ring_South	-	800	0.20	2.30	2.50
ASL_Block	1300-1800	500	0.00	2.50	2.50
Ring_West	-	800	0.19	2.40	2.59
Ring_East	-	800	0.14	2.40	2.54
Upper_Middle_Intrusive_West	-	600	0.24	2.40	2.64
Upper_Middle_Intrusive_East	-	600	0.18	2.40	2.58
Middle_Intrusive_West	-	1100	0.19	2.40	2.59
Middle_Intrusive_East	-	1100	0.20	2.40	2.60
Lower_Intrusive	1800-3800	2000	0.11	2.50	2.61
WestFlank_Intrusive	2600-6800	4300	0.16	2.50	2.66
Rift_Zone	(-3800)- (-6800)	3000	0.18	2.50	2.68

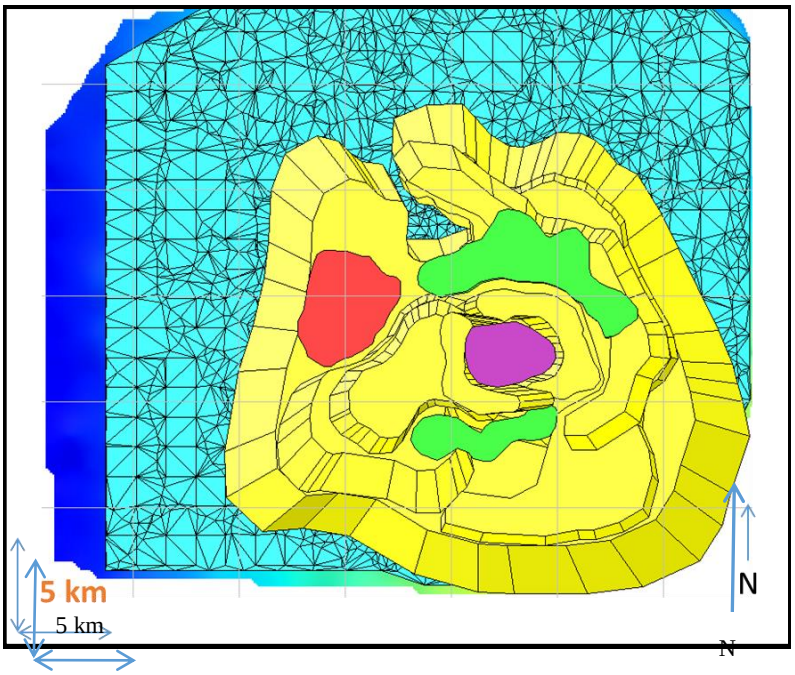

Figure 6. The higher density bodies seen from above responsible of the main observed gravity anomalies. Colors correspond to the formation and density values given in Table 1.

These results are also represented by a cross-section and a 3-D perspective view in figure 7.

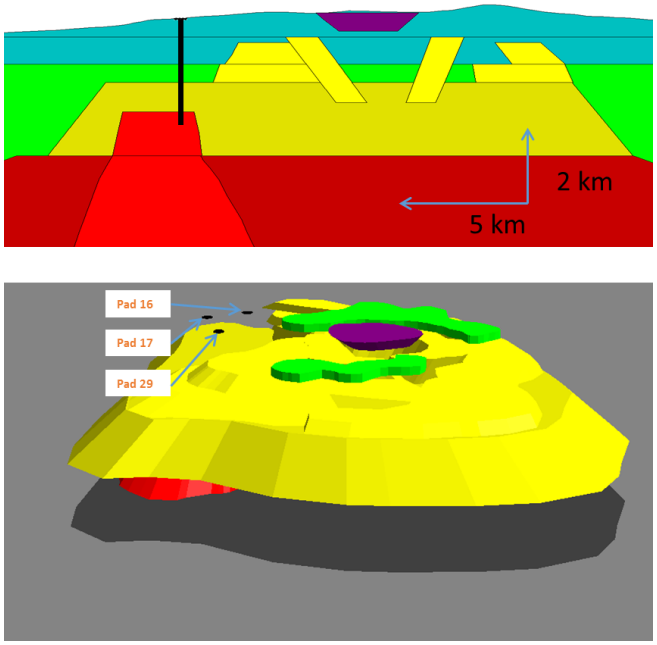

Figure 7. A cross section through well NWG55-29 on Pad 29 (upper plot) and 3D perspective view (lower plot) of the higher density bodies responsible of the main observed gravity anomalies. Colors correspond to the formation and density values given in Table 1.

Final gravity data residuals (Figure 8) show that most of the observed gravity data can be explained by the modeled gravity bodies. The inversion attempts to minimize the errors for all of the data and the residual map illustrates that the gravity residual is in general slightly positive in the center of the area and negative toward the western edge of the domain. Edge effect artifacts can be seen on the periphery and are due to truncation of the model domain. An improved fit to the center of the area can be obtained by slightly increasing the density of all modelled bodies but will cause the western negative residual to become more pronounced. Overall, the inversion results provide good fits to the gravity data and are consistent with previous gravity modeling results (Frone et al, 2015) and other site characterization information.

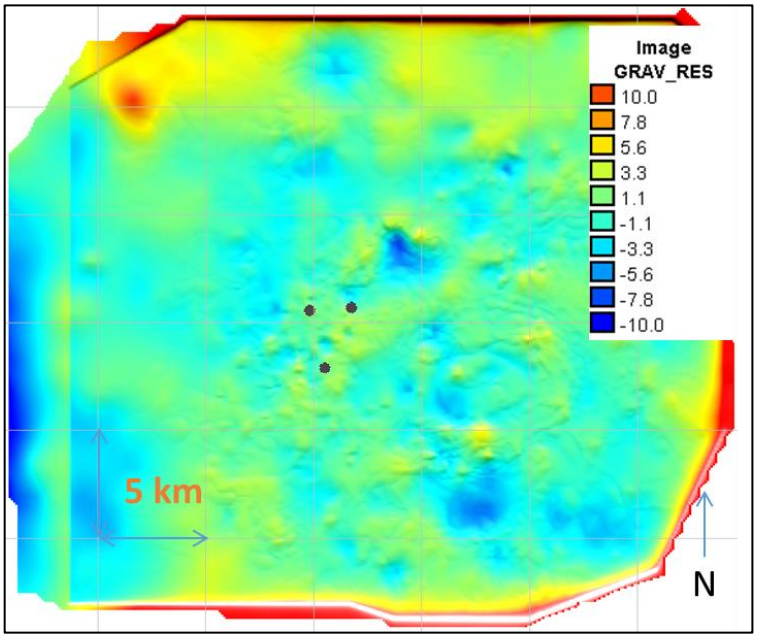

Figure 8. Final data residual map showing the difference between modeled and observed gravity data. Color map units are in mGal.

The density log for well NWG 55-29 is shown in Figure 9 along with average density values at specific depths and the values obtained from the gravity inversion results. Modeled bodies are in reality a composite of thin layers; however, average densities of the modeled gravity bodies are generally consistent with the density/lithology observed from well logs.

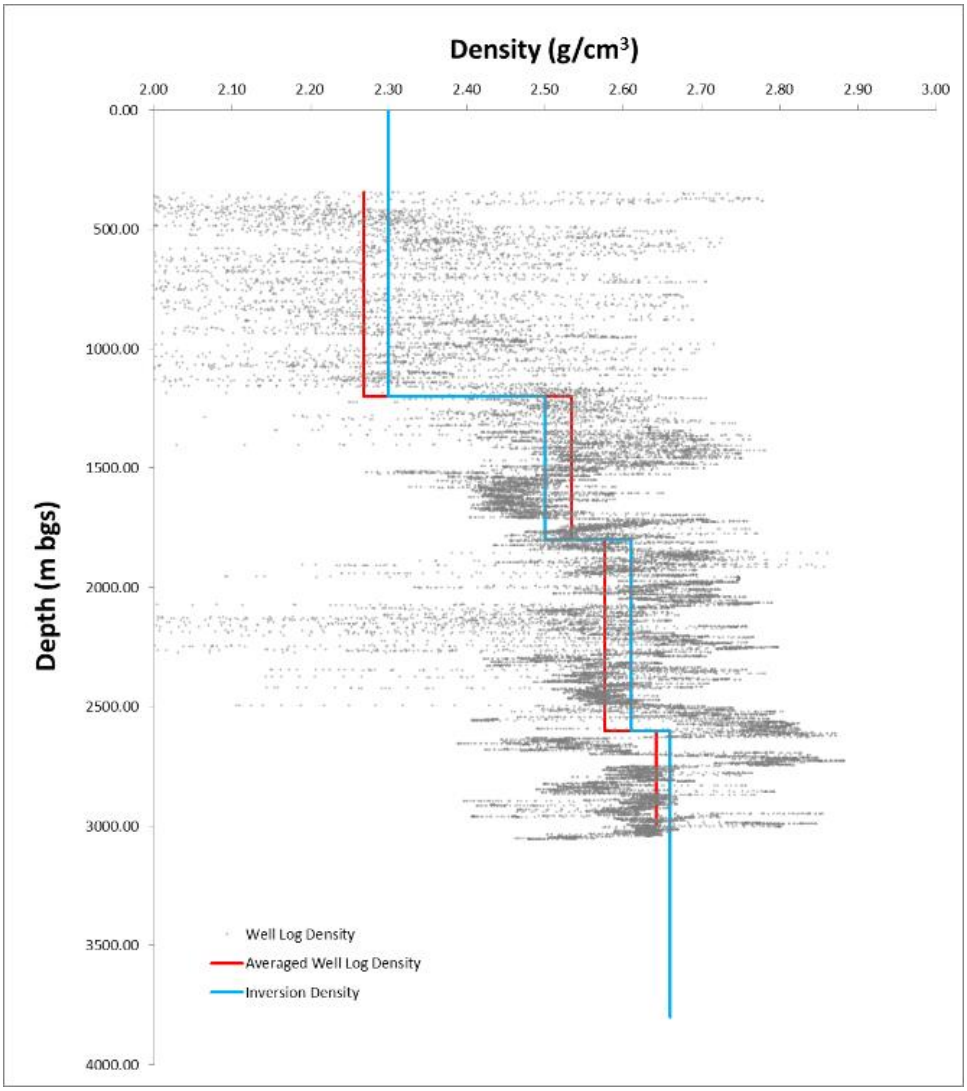

Figure 9. Well NWG 55-29 density log (gray points) along with an averaged log density (red) over specific depths intervals and a comparison to the density values obtained from the gravity inversion (blue).

Another representation of the main density bodies is shown in Figure 10. The "West Flank Intrusive" is in the center, as identified in Table 1 (density 2.66 g/cm^3; 0.16 gm/cm^3 above surrounding formation density). The "Ring East" unit from Table 1 is displayed on the right (density 2.54 gm/cm^3; 0.14 gm/cm^3 above surrounding formation density). The colored dots are the microseism locations from the 2014 deep EGS stimulation.

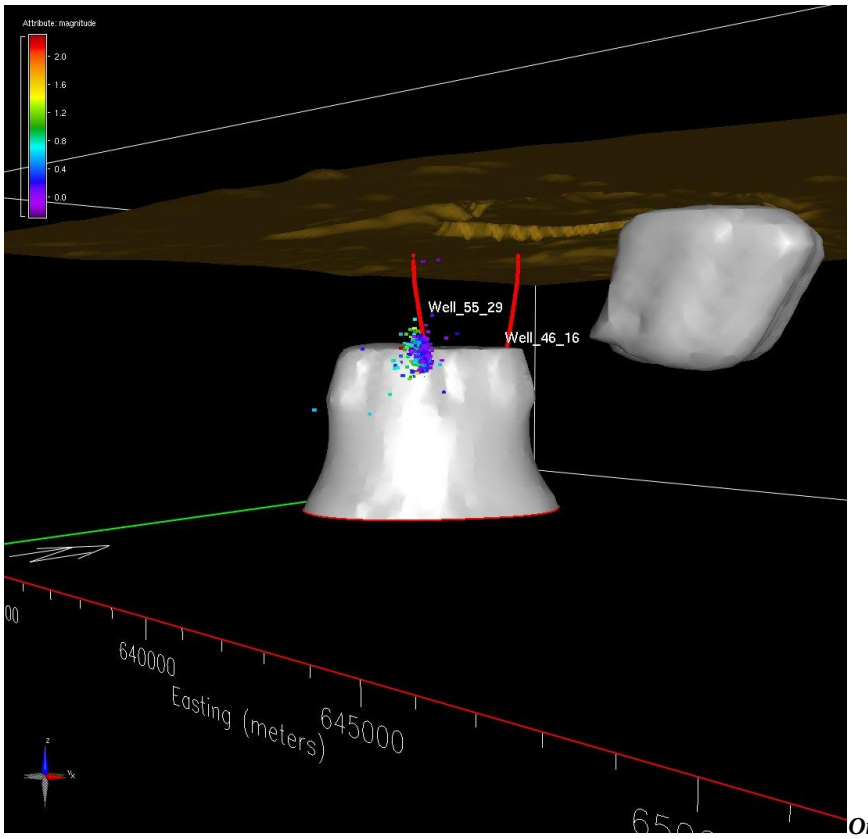

On F

Figure 10. Two main geophysical units defined by density from 3D gravity inversion showing two wells NWG 55-29 and NGW 46-16 with the cluster of microseisms from the 2014 NEGSD stimulation displayed. The view is westward looking and the Newberry Volcano caldera can be seen from below in the topographical layer colored in dark yellow.

Note that the cluster of microseisms from the 2014 EGS stimulation at well NWG 55-29 appears to conform approximately to the boundary of the West Flank Intrusive. The West Flank Intrusive's northern and eastern boundaries approximately overlap the region of higher resistivity at depth beneath the west flank, as delineated by the MT derived 3D resistivity model (Mark-Moser et al., 2016). The possibility that the eastern boundary of the gravity and the MT anomalies that we associate with this intrusive body could be an artifact of sparser data coverage proximal to the western rim of the caldera and interior to the east of the NEWGEN FORGE site has been considered. While the spatial resolving power of both MT and gravity methods will be lower toward and inside of the caldera because of the sparser sampling there, stations to the immediate east of the FORGE site are sufficient to delineate the eastern boundary of both density and resistivity anomalies; consequently. This is not taken to be an artifact of station coverage, but a deep structural boundary. Whether the clustering of microseisms along this intrusive body's boundary is coincidental to the location of NWG 55-29, or reflects a physical constraint on the local stress field will require additional site characterization and modeling to determine.

5. CONCLUSION

Using the initial structures discovered by seismic tomography, inversion of gravity data has been performed. Shape, density values and depths of various bodies were allowed to vary and three main bodies have been identified. Densities of the middle and lower intrusive bodies (~2.6-2.7 g/cm3) are consistent with rhyolite, basalt or granites. Modeled density of the near-surface caldera body match that of a low density tephra material and the density of the shallow ring structures contained in the upper kilometer correspond to that of welded tuff or low-density rhyolites. Modeled bodies are in reality a composite of thin layers; however, average densities of the modeled gravity bodies are in good agreement with the density log obtained in one well located on the western flank (well 55-29). Final gravity data residuals show that most of the observed gravity anomalies at the surface can be explained by the modeled gravity bodies and are consistent with other site characterization information.

ACKNOWLEDGEMENTS

This research has been conducted in the framework of the Newberry FORGE Phase 1 project supported by the Department of Energy under Award Number DE-EE 0007158.

REFERENCES

Beachly, M.W., E.E.E. Hooft, D.R. Toomey, and G.P. Waite. "Upper crustal structure of Newberry Volcano from P-wave tomography and finite difference waveform modeling." *Journal of Geophysical Research* 117(B10311):17 (2012).

Cladouhos, T. T., S. Petty, M. W. Swyer, M. E. Uddenberg, K. Grasso, and Y. Nordin: Results from Newberry Volcano EGS Demonstration, 2010–2014, Geothermics, doi: http://dx.doi.org/10.1016/j.geothermics.2015.08.009 (2016).

Clouard, V., A. Bonneville and H. Barsczus H., Size and depth of frozen magma chambers under atolls and islands of French Polynesia using detailed gravity studies, *J. Geophys. Res., 105, 8173-8193 (*2000).

Donnelly-Nolan and R.A. Jensen: Ice and water on Newberry Volcano, central Oregon, in Volcanoes to Vineyards: Geologic Field Trips through the Dynamic Landscape of the Pacific Northwest, J.E. O'Connor, R.J. Dorsey, and I.P. Madin (eds.), GSA Field Guide 15, 81-90 (2009).

Frone, Z. Heat flow, termal modeling and whole rock geochemistry of Newberry Volcano, Oregon and heat flow modeling of the Appalachian Basin, West Virginia. Dissertation thesis, Southern Methodist University (2015).

Frone, Z., A. Waibel, and D. Blackwell: Thermal Modeling and EGS Potential of Newberry Volcano, Central Oregon. PROCEEDINGS, Thirty-Ninth Workshop on Geothermal Reservoir Engineering, Stanford University, Stanford, California, February 24-26 (2014).

Jensen, R.A.: Roadside Guide to the Geology of Newberry Volcano, 4th Edition, 182 p (2006).

MacLeod, N.S., D.R. Sherrod, and L.A. Chitwood: Geologic map of Newberry Volcano, Deschutes, Klamath, and Lake Counties, Oregon. USGS Open-File Report 82-847, 27 p. (1982).

MacLeod, N.S., D.R. Sherrod, L.A. Chitwood, and R.A. Jensen. Geologic Map of Newberry Volcano, Deschutes, Klamath, and Lake Counties, Oregon. U.S. Geological Survey, 2 sheets, scale 1:62,500, pamphlet, 523 p, scale 1:62,500 (1995).

Mark-Moser, M., J. Schultz, A. Schultz, B. Heath, K. Rose, S. Urquhart., E. Bowles-Martinez, and P. Vincent: A Conceptual Geologic Model for the Newberry Volcano EGS Site in Central Oregon: Constraining Heat Capacity and Permeability through Interpretation of Multicomponent Geosystems Data, Proceedings: Forty-first Workshop on Geothermal Reservoir Engineering, Stanford University, Stanford, CA, Feb 20-22, (2016).

NEWGEN, Phase 1 FORGE Topical Report and Appendices, https://energy.gov/eere/forge/downloads/pacific-northwest-national-laboratory-phase-1-report, (2016).

Priest, G.R. 1990. Volcanic and Tectonic Evolution of the Cascade Volcanic Arc, Central Oregon. *Journal of Geophysical Research* 95(B12):19.583–19.599.

Roberts, C.W., R.P. Kucks, and P.L. Hill. 2008. Oregon magnetic and gravity maps and data–A website for distribution of data. U.S. Geological Survey Data Series 355.

Robinson, P.T., G.F. Brem, and E.H. McKee: John Day Formation of Oregon: A Distal Record of Early Cascade Volcanism. Geology, v. 12(4), 229-232 (1984).

Waibel, A.F., Z.S. Frone, and D.D. Blackwell. Geothermal exploration of Newberry Volcano, Oregon, Final Report for the DOE Innovative Exploration Technology (IET) Grant 109 program supporting geothermal exploration of Newberry Volcano, Oregon. Final report for DOE Award: DE-EE0002833 (2015)

Zonge (Zonge Geosciences, Inc.). 2007. Gravity survey on the Newberry project, Deschutes County, Oregon, for Davenport Resources LLC, Data Acquisition Report, 38 pp.

Zonge (Zonge Geosciences, Inc.). 2010. Gravity survey on the Newberry project, Deschutes County, Oregon, for Davenport Resources LLC, Data Acquisition Report, 41 pp.

Zonge (Zonge Geosciences, Inc.). 2012. Gravity survey on the Newberry project, Deschutes County, Oregon, for Davenport Resources LLC, Data Acquisition Report, 40 pp.